# Predicting the final collective mode for Kuramoto rotators in a ring-like topology

Károly Dénes[1], Sándor Bulcsú[1,2] and Zoltán Néda[1]
[1] *Babeş-Bolyai University, Department of Physics, Cluj, Romania*
[2] *Goethe University Frankfurt, Institute for Theoretical Physics, Frankfurt am Main, Germany*

November 16, 2017

**Abstract**

Stationary collective modes in a ring of identical and locally coupled Kuramoto-type rotators are investigated. We show that the final stationary collective mode is predictable after a $t_s$ time in the dynamics. A simple method is given for determining this $t_s$ time-moment. For randomly chosen initial conditions we study numerically the scaling of the mean $t_s$ value as a function of system size and coupling parameter between the rotators.

## 1 Introduction

Collective behavior in ensembles of interacting oscillators is one of the oldest problems in the field of dynamical systems and statistical physics [1, 2]. Interestingly however, this field is still active, raising new problems [3], revealing further surprises [4] and offering applications and modeling tools for many other areas of science and engineering [5].

Synchronization of non-identical and coupled oscillators is an intriguing fact observed in many real systems. The Kuramoto model [6] is probably the most widely studied system for modeling such synchronization phenomena. For globally coupled rotators it exhibits an order-disorder transition, which is useful to explain emerging synchronization in physical, social or biological systems [7]. By varying the characteristics of the interactions acting between the rotators, many variants of the original model were studied analytically and numerically. It was found that the topology of the interaction determines the nature of the emerging collective behavior. In such sense the Kuramoto model was considered both on regular and random graphs [8, 9, 10] using interactions between neighbors of different order [11, 12]. The model was generalized also by considering a mixture of attractive and repulsive couplings [13]. In general, for locally coupled nonidentical oscillators it was found a rich variety of collective behavior: frequency locking, phase synchronization, partial synchronization or incoherence. Time-delay in the interactions between the active neighbors introduces an extra complexity in the Kuramoto model by drastically increasing its dimensionality [14, 15, 7, 3]. It yields also new surprises in large oscillator ensembles, by generating novel, long lived transient states where some of the oscillators synchronized while the others remained completely disorganized. Such states were named as "chimera" states, and they were observed in many different coupling topologies [16, 3, 4]. Nowadays it is believed that the condition to get such "chimera" states in interacting oscillator ensembles is to have some sort of non-uniformity in the coupling strength, in the oscillators natural frequencies or in the time-delay. Here we do not consider inhomogenities or time delay so chimera-like states are not expected to appear.

The system investigated by us consist of $N$ classical Kuramoto oscillators in a ring-like topology, with identical intrinsic frequencies $\omega_0$, each oscillator being coupled to its nearest neighbors with coupling strength $K$. The dynamics of the system is given by the coupled first order differential equation system:

$$\dot{\theta}_i = \omega_0 + K[\sin(\theta_{i-1} - \theta_i) + \sin(\theta_{i+1} - \theta_i)]\,, \qquad (1)$$

with $\theta_i = \theta_i(t)$ being the time-dependent phase of the $i$-th oscillator, $i = \overline{1, N}$, together with the periodic boundary conditions $\theta_{N+1} = \theta_1$ and $\theta_0 = \theta_N$. The symmetry of the system allows many dynamically stationary states (different types of collective behavior) to appear [12, 17]. Such states are generalized synchronization states in form of self-closing traveling waves with a fixed winding number, $m$, all the oscillators having the same $\omega_0$ frequency. The simplest and most probable state is the classical synchrony ($m = 0$) where all rotators move in phase. The other stationary states ($m = \pm 1, \pm 2...$) are characterized by a locked phase-difference between the neighbors. Our aim here is to estimate the average time necessary for selecting the final state starting from randomly chosen initial phases. By the selection time we mean the shortest time after which we can predict the final stationary state of the system.

In our numerical study we fix the $T_0 = 2\pi/\omega_0 = \pi$ natural period for the oscillators (defining by this the time-unit), and study the influence of the remaining $N$ and $K$ parameters on the selection time.

## 2 Overview of the known results

Here we give an overview in an original approach of the known results for the stationary states and introduce also some basic concepts and notations that are used in the following sections.

## Stationary states

For convenience reasons we switch to a reference frame rotating with the natural frequencies of the oscillators:

$$u_i(t) = \theta_i(t) - \omega_0 t. \tag{2}$$

The equation of motion in the rotating frame will be:

$$\begin{aligned} \dot{u}_i = K[\sin(u_{i-1} - u_i) + \sin(u_{i+1} - u_i)] = \\ = F(u_{i-1}, u_i, u_{i+1}) \end{aligned} \tag{3}$$

In this frame equation (3) is a gradient system having the following potential function [12]:

$$V = -\frac{K}{2} \sum_{j=1}^{N} \left(\cos(u_{j-1} - u_i) + \cos(u_{j+1} - u_i)\right). \tag{4}$$

Equation (3) is now equivalent to $\dot{u}_i = -\partial V / \partial u_i$. Being a gradient system means that the stationary states are always fixpoints while limit cycles or any kind of different attractors are not allowed [**?**]. These stationary states correspond to local minima, maxima or saddle points of $V$.

Fixpoints require $\dot{u}_i = 0$, hence:

$$K[\sin(u_{i-1} - u_i) + \sin(u_{i+1} - u_i)] = 0. \tag{5}$$

Converting this sum to a product will yield:

$$K \sin\left(\frac{u_{i+1} - 2u_i + u_{i-1}}{2}\right) \cos\left(\frac{u_{i+1} - u_{i-1}}{2}\right) = 0. \tag{6}$$

If either of the two trigonometric functios evaluates to 0 we have stationarity. Thus the two conditions are:

$$u_{i+1} - 2u_i + u_{i-1} = 2k_i\pi, \quad k_i \in \mathbb{Z}, \tag{7}$$

and

$$u_{i+1} - u_{i-1} = (2q_i + 1)\pi, \quad q_i \in \mathbb{Z}. \tag{8}$$

The above conditions can be satisfied for the whole system in the following manners:

(a) condition (7) is fulfilled for all $i$ indeces

(b) condition (8) is true all over the system.

(c) for some $i$ values condition (7) holds, while for the other $i$ values condition (8) is true

While cases (a) and (b) conserve the symmetry of the system, case (c) will violate it, corresponding to a nontrivial symmetry breaking.

To represent the state of the system on a unit circle it is convenient to use a new phase parameter: $\phi_i$ $(0 \le \phi_i < 2\pi)$:

$$\phi_i = u_i \mod 2\pi\,. \tag{9}$$

Taking into account that the asymptotic solutions are characterized with fixed $u_i$ values, these are phase-locked states. Therefore the relative positions of oscillators $i$ and $i-1$ on the unit circle has to be characterized with a parameter $\Delta\phi_i$, named hereafter as *phase shift* between oscillators $i$ and $i-1$, which takes values between $-\pi$ and $\pi$ as it is illustrated in Fig. 1. In order to achieve this, the $\Delta\phi_i$ parameter has to be defined as:

$$\begin{aligned} \Delta\phi_i &= \phi_i - \phi_{i-1} \quad \text{for} \quad -\pi \le \phi_i - \phi_{i-1} < \pi \\ \Delta\phi_i &= \phi_i - \phi_{i-1} - 2\pi \quad \text{for} \quad \pi \le \phi_i - \phi_{i-1} < 2\pi \\ \Delta\phi_i &= \phi_i - \phi_{i-1} + 2\pi \quad \text{for} \quad -2\pi < \phi_i - \phi_{i-1} < -\pi \end{aligned} \tag{10}$$

which can be written in a compact form by using the floor function ($f(x) = \lfloor (x) \rfloor$):

$$\Delta\phi_i = (\phi_i - \phi_{i-1}) - 2\pi \left\lfloor \frac{\phi_i - \phi_{i-1} + \pi}{2\pi} \right\rfloor. \tag{11}$$

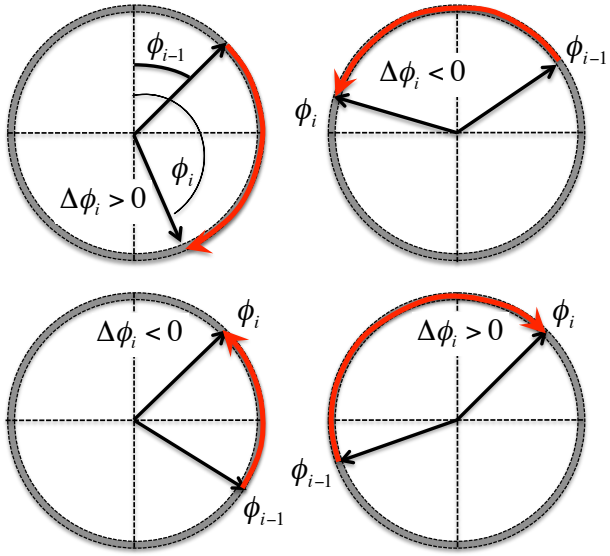


**Figure 1:** (color online) Illustration of the $\Delta\phi_i$ phase differences, see also Eqs. (10)

Let us consider now $\Delta_N = \sum_{i=1}^{N} \Delta\phi_i$. Using Eq. (11), we can write

$$\Delta_N = \sum_{i=1}^{N} (\phi_i - \phi_{i-1}) - 2\pi \sum_{i=1}^{N} \left\lfloor \frac{\phi_i - \phi_{i-1} + \pi}{2\pi} \right\rfloor \tag{12}$$

In our ring topology $\phi_0 = \phi_N$, so the first sum in Eq. (12) is zero. Since the terms in the second sum are all 0 or $\pm 1$, it results that the second sum should be an integer, $m \in \mathbb{Z}$. As a consequence the sum of the phase shifts satisfy the relation (see also [17]):

$$\Delta_N = 2\pi m, \tag{13}$$

where negative values of $m$ are also allowed. This relation has nothing to do with the dynamical equations of the system, it is solely a consequence of the imposed topology.

Considering case (a) for the fix point condition, we rewrite equations (7) using the $\phi_i$ variables:

$$\phi_{i+1} - 2\phi_i + \phi_{i-1} = 2k_i\pi, \quad k_i \in \mathbb{Z}. \tag{14}$$

Regrouping the multiples of $2\pi$ one can write the above condition also in terms of the phase shifts:

$$\Delta\phi_{i+1} - \Delta\phi_i = 2l_i\pi, \quad l_i \in \mathbb{Z} \tag{15}$$

Since $\Delta\phi_i \in [-\pi, \pi)$ this condition is fulfilled only for $l_i = l = 0$. Hence:

$$\Delta\phi_{i+1} = \Delta\phi_i. \tag{16}$$

Consequently, in these stationary states $\Delta\phi_i = \Delta\phi$, constant for all oscillator pairs. This leads to the result:

$$\Delta\phi = \frac{\Delta_N}{N} = 2\frac{m}{N}\pi\,. \tag{17}$$

Due to the fact that the phase shift satisfies $-\pi \leq \Delta\phi < \pi$, we get that $-N/2 \leq m < N/2$, with $m \in \mathbb{Z}$. Stationary states stemming from equation (18) are defined thus by the $m$ number, referred from now on as the *state index* or *winding number*. Synchrony in the classical sense corresponds to the 0 index, the other states being indexed from $-N/2$ up to $N/2-1$. The existence of these stationary states is well-known in the literature [18, 12, 17], however other authors use different arguments to arrive at this result.

The other branch of stationary states given by case (b) is obtained by satisfying the condition in equations (8). With the same reasoning as in case (a) one arrives to:

$$\Delta\phi_{i+1} + \Delta\phi_i = (2p_i + 1)\pi, \quad p_i \in \mathbb{Z} \tag{18}$$

Taking into account that $\Delta\phi_i \in [-\pi, \pi)$ the two phase shifts can only add up to $\pm\pi$ which is equivalent to $p_i \in \{-1, 0\}$. Generally the $p_i$ parameter may be different for the pairs of rotators, however it can be shown that it is constant over the whole system. In order to realise this, let us assume that the $p_i$ value changes for two consecutive pairs:

$$\begin{aligned} \Delta\phi_{i+2} + \Delta\phi_{i+1} &= \pm\pi \\ \Delta\phi_{i+1} + \Delta\phi_i &= \mp\pi. \end{aligned} \tag{19}$$

Subtracting the two equations we get:

$$\Delta\phi_{i+2} - \Delta\phi_i = \pm 2\pi. \tag{20}$$

This condition cannot be fulfilled since $-\pi \leq \Delta\phi_i < \pi$ so the difference between two phase shifts is always greater than $-2\pi$ and smaller than $2\pi$, therefore $p_i = p_{i+1} = p$ ($p_i \in \{-1, 0\}$) for all pairs.

To gain some more information about this type of states we sum up all the equations in (19):

$$\sum_{i=1}^{N} \Delta\phi_{i+1} + \Delta\phi_i = \sum_{i=1}^{N} (2p + 1)\pi. \tag{21}$$

Invoking the periodic boundary condition we can write:

$$2\sum_{i=1}^{N} \Delta\phi_i = 2 \cdot 2m\pi = N(2p + 1)\pi. \tag{22}$$

Finally by using $p = \pm 1$ we determine the possible values of the $m$ winding number:

$$m = \pm\frac{N}{4}. \tag{23}$$

These kind of states are only possible if $N$ is divisible by 4 and their number is infinite since there are infinite phase shifts for which the $\Delta\phi_{i+1} = \pm\pi - \Delta\phi_i$ condition holds.

The symmetry violated case (c) is a combination of conditions (18) some $i$ values and (19) with $p_i \in \{-1, 0\}$, for the other $i$ indices. Since this is a highly unusual case, we present an example of such a nontrivial configuration for $N = 4$ oscillators in Fig. **??**.

One can immediately realise that there are many possibilities to fulfil case (c). Following a similar argument as the one used in case (b) one can show that if there are triplet of oscillators satisfying condition (19) all of them must have the same $p_i = p$ ($p_i \in \{-1, 0\}$) value. As a consequence of these all $\Delta\phi_i$ values are either a constant $\Delta\phi$ or $(2p + 1)\pi - \Delta\phi$. Assuming that there are $n$ number of $\Delta\phi_i = \Delta\phi$ phase shifts and consequently $N-n$ phase shift with $(2p+1)\pi-\Delta\phi$ value, the imposed boundary condition (13) leads to

$$\sum_{i=1}^{N} \Delta\phi_i = n\,\Delta\phi + (N - n)\,[(2p + 1)\pi - \Delta\phi] = 2m\pi, \tag{24}$$

where $-N/2 \leq m < N/2$ with $m \in \mathbb{Z}$.

## Stability of the stationary states

In case (a) when condition (7) is fulfilled for all $i$ indeces using the condition in (17) we identified the possible stationary states characterised by equal phase-shifts $\Delta\phi = 2m\pi/N$ with $-N/2 \leq m < N/2$. We analyze now their stability. For this purpose we use the standard linearization near the equilibrium point . The Jacobian of the system, evaluated at the equilibrium solution $\mathbf{u}^* = (u_1^*, \dots, u_i^*, \dots)$ is constructed as follows:

$$\begin{aligned} \left.\frac{\partial F(u_{i-1}, u_i, u_{i+1})}{\partial u_j}\right|_{\mathbf{u}^*} = K\Big[ &\cos(u_{i-1}^* - u_i^*)\delta_{i-1,j} - \\ &-\Big(\cos(u_{i-1}^* - u_i^*) + \cos(u_{i+1}^* - u_i^*)\Big)\delta_{i,j} + \\ &+\cos(u_{i+1}^* - u_i^*)\delta_{i+1,j}\Big]. \end{aligned} \tag{25}$$

In equilibrium $u_i^* - u_{i-1}^* = \Delta\phi$. Hence, we can write the Jacobian explicitely in the form of a circulant matrix:

$$\left.\frac{\partial F}{\partial u_j}\right|_{\mathbf{u}^*} = K\cos\Delta\phi \begin{pmatrix} -2 & 1 & 0 & \dots & 0 & 0 & 1 \\ 1 & -2 & 1 & \dots & 0 & 0 & 0 \\ 0 & 1 & -2 & \dots & 0 & 0 & 0 \\ \vdots & \vdots & \vdots & \ddots & \vdots & \vdots & \vdots \\ 0 & 0 & 0 & \dots & -2 & 1 & 0 \\ 0 & 0 & 0 & \dots & 1 & -2 & 1 \\ 1 & 0 & 0 & \dots & 0 & 1 & -2 \end{pmatrix} \tag{26}$$

The eigenvalues of this matrix can be written in an explicit form [19]:

$$\lambda_j = -2K\cos\Delta\phi\left(1 - \cos\frac{2\pi j}{N}\right), \qquad j = \overline{0, N-1} \tag{27}$$

The expression in the bracket is non-negative, so in order to have a stable equilibrium we need $\cos\Delta\phi > 0$, which implies:

$$-\frac{\pi}{2} < \Delta\phi < \frac{\pi}{2}. \tag{28}$$

This result can be formulated in terms of the state index:

$$-\frac{N}{4} < m < \frac{N}{4}. \tag{29}$$

This is the same results as the one given in [17].

Following a similar argument in case (b) (condition (8) is true all over the system) one can show that the eigenvalues of the Jacobian are all zero, therefore the fixpoints have neutral stability. Details are given in the Appendix.

Case (c) is more complicated and we have exact analytical results only for some special choices of the parameters. These results indicate that the fix points are unstable. For more details please see the Appendix. For other situations our computer experiments supports the same conclusion.

In Conclusion....

## Computer experiments

Numerical integration of the system of equations (1) starting from uniformly distributed initial $\theta_i$ values will reveal only the stable stationary states. It worth noting that a uniform distribution of the states in the $\theta$ space will lead to a uniform distribution in the $\Delta\phi$ space as well.

A series of simulations performed on systems with sizes ranging from $N = 4$ to $N = 100$ confirms the results presented in equations (13) and (29). In agreement with the simulation results presented in [12] we also find that for $-\frac{N}{4} < m < \frac{N}{4}$ the probability distribution of the stable states can be described with a Gaussian envelope curve (Fig. 2). As it is visible in the inset of Fig. 2, the standard deviation of the probability distribution scales linearly with the square-root of the system size, a result emphasized already in [12]. Our computer experiments also proved that the distribution does not change if one changes the coupling strength $K$.

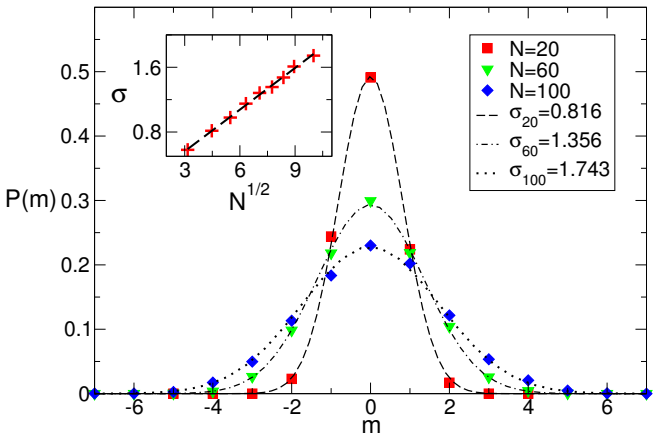


**Figure 2:** (color online) Probability distribution of the final states for different oscillator numbers $N$, and the normalized Gaussian probability density envelope curve fitting the discrete points. The inset shows the scaling of the standard deviation, $\sigma \propto \sqrt{N}$. The distributions are obtained over 5000 runs for the $K = 1.5$, $\omega_0 = 2$ parameters.

# 3 Dynamics of the system

Let us consider first the evolution of the system in the $N$ dimensional $\Delta\phi$-space. Since $\Delta\phi_i$ is defined for $-\pi \leq \Delta\phi_i < \pi$ the allowed phase space is confined in a hypercube centered in the origin of the $N$-dimensional space (for the 3D case see Fig. 3). In the stationary states all phase shifts are equal, so the attractors lie on the main diagonal of the hypercube (large black points in Fig. 3) . We have shown that these states are discrete, thus the attractors represent distinct points on this line. In Section 2, Eq. (13), we have also proved that at each time moment of the dynamics:

$$\sum_{i=1}^{N} \Delta\phi_i = 2m\pi \tag{30}$$

with $-N/2 \leq m < N/2$ and $m \in \mathbb{Z}$. Equation (30) can be interpreted as the equation of a plane in the $N$-dimensional space, determined by the phase shifts in the system. The $N$-dimensional characteristic point of the system can only exist on the planes defined by various $m$ values in (30). These planes are parallel to each other, and as $m$ increases in absolute value the area of the cross-sections of the planes and the hypercube gets smaller. The 3D case is illustrated in in Fig. 3, where the larger central plane is for $m = 0$, and the the two smaller planes are for $m = \pm 1$. During the evolution of the system the characteristic point is moving on these planes. Jumps between the planes are also possible when the configuration of the phase shifts changes in a way that the winding number defined by the sums (see Eqs. (12) and (13)) is altered by +1 or -1. Sometimes this occurs when the characteristic point of the system reaches the boundary of a plane (i. e. phase shift between two oscillators crosses the $\pi$ or -$\pi$ value). This representation gives a first qualitative image for the dynamics of the oscillator ensemble.

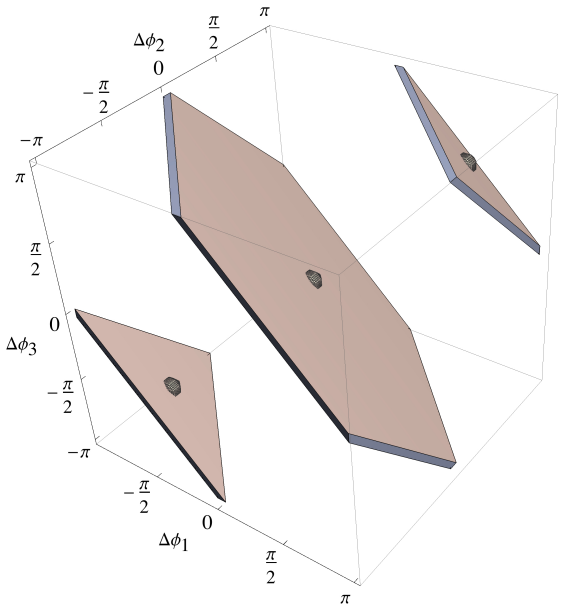


**Figure 3:** (color online) The planes defined by condition (3) for a system of $N = 3$ rotators. Black spheres indicate the allowed stationary states of the system. The central large plane is for $m = 0$, while the other two planes are for the $m = \pm 1$ states.

For $N > 3$ the actual trajectories cannot be easily visualized. In order to get some useful information on the dynamics of the system one option is to plot the phase-shifts between each nearest-neighbor oscillator $\Delta\phi_i$ as function of time. A characteristic time-evolution is sketched in Fig. 4. One can observe on the plotted dynamics the jumps that occur at the border of the planes (either jumping on an other edge of the plane, or jumps to another plane). From such a representation is not evident the time-moment at which one is already able to predict the final state. Our aim in the following sections is to give a useful numerical method that allows such a prediction. In Fig. 4 we sketched by the red line the time moment at which our prediction works (see Section 5).

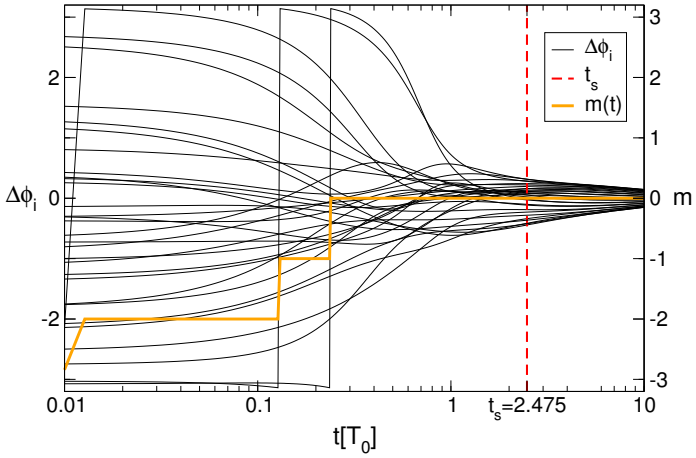


**Figure 4:** (color online) Characteristic time evolution for the phase-differences $\Delta\phi_i$ between neighboring oscillators. The dashed red line indicates the time moment for the selection of the final state for $N = 30$, $K = 0.75$ (see the next section). Note the logarithmic time-scale.

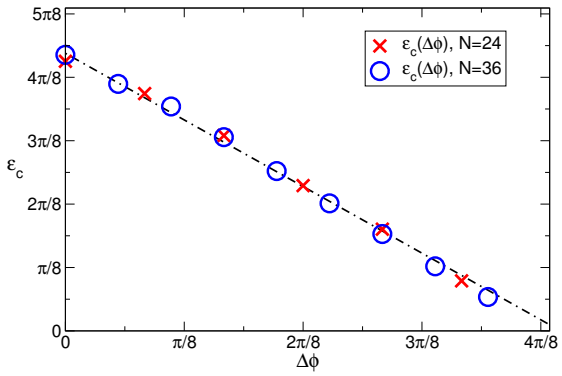


**Figure 5:** (color online) The radius $\epsilon_c$ of the compact attraction basins around different stationary states for two different system size, $N$. The results are plotted as a function of the phase difference in the stationary states, since in such case the trends for different $N$ values overlap. For the definition of $\epsilon_c$ see the text. The values of $\epsilon_c$ are estimated on an ensemble of 1500 initial states, obtained for $K = 10$ and fitted by the line $\epsilon_c = 1.7195 - 1.0501\Delta\phi$.

## 4 Compact basin of attractions around the stationary state

One can also investigate the size of the compact basin of attraction around a stationary state $m$. Starting from inside this domain the dynamics will converge to the stationary state $m$. Using the picture introduced in the previous section for these compact basins of attraction, the dynamics is confined to the plane corresponding to mode $m$, never jumping actually to other planes. In such case the final state is predictable right from the starting moment. In order to estimate the a size of these domains, one considers the stationary states with fixed $m$ value: $\theta_i^* = i \cdot 2m\pi/N$. We perturb these states, $\theta_i = \theta_i^* + \xi$, with uniformly distributed $\xi \in [-\epsilon, \epsilon)$ random variables ($\epsilon \in [0, \pi]$) and determine the largest value $\epsilon_c$ so that the dynamics starting from the initial state $\theta_i$ will always converge to state $m$. Results for the $\epsilon_c$ values computed for two different system sizes, $N = 24$ and $N = 36$, are plotted in Fig. 5.

The probability that a randomly selected initial state from the whole $N$-dimensional hypercube of volume $(2\pi)^N$ is inside this compact attraction basin, where the final state is predictable right from the beginning, is hence:

$$P_{\rm comp} \leq \left(\frac{2\epsilon_c}{2\pi}\right)^N \approx \left(\frac{1.7 - \frac{2m\pi}{N}}{\pi}\right)^N . \qquad (31)$$

The approach given for $P_{\rm comp}$ (last part of Eq. (31)), results from the fact that $\epsilon_c$ decreases linearly as a function of $\Delta\phi$, independently of the system size. This is proven by the results plotted in Fig. 5. Even for a relatively small system size, e. g. $N = 8$, the probability that a randomly selected initial state is in the largest compact basin of attraction around the $m = 0$ is: $P_{\rm comp} < 0.01$.

## 5 Predicting the final stationary state

It is a natural question now, how and when we are able to predict the final stationary state, if the system is initially out of the compact attractor region around the stationary state. Similarly to the known Kuramoto order parameter $r_0$ (for $m = 0$), one can define a generalized order parameter $r_m \in [0, 1]$ for each $|m| > 0$ stationary state. This parameter will give a useful information on how well the system approached the given stationary state with index $m$:

$$r_m(t)e^{i\psi_m(t)} = \frac{1}{N}\sum_{j=1}^{N} e^{i[\theta_j(t) - (j-1)\frac{2m\pi}{N}]}. \qquad (32)$$

Naturally for $r_m = 1$, the system is in the stationary state characterized by the index $m$. The smaller $r_m$ is, the further the system is from this stationary state. This generalized order parameter is a useful tool for following the time-evolution of the system.

Characteristic results for the time evolution of the $r_m$ values are shown in Fig. 6. One can split the plotted evolution curves in two regions, as it is done by the vertical dashed line. In the first stage, $t < t_s$, several order parameters are increasing, while in the second stage, $t \geq t_s$, only the $r_m$ corresponding to the selected state keeps increasing. We have proved on thousands of samples that once such a situation is reached, for $t > t_s$, it remains stable (i. e. this order parameter will continue to growth and the others will converge to zero). Such a turning point will always arise, hence by detecting it one can already predict the final state of the system. It is interesting to note that the appearance of stage two is possible also when the growing order parameter is relatively small, and one would not even expect that the corresponding state is the one where the system converges.

On Fig. 4 we also indicated this $t_s$ time moment for the same run. One can see that in the dynamics of $\Delta\phi_i$ is definitely not obvious that this is the turning point for predictability.

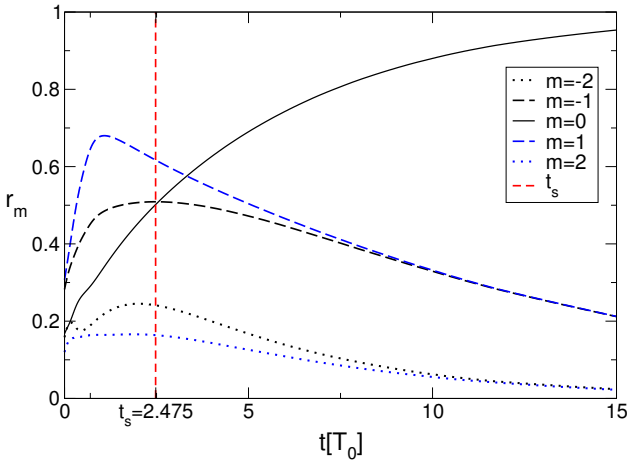


**Figure 6:** (color online) Characteristic time-evolution for the order parameters of different final states, $r_m$ as a function of time. For avoiding the overcrowding of the graph we have plotted only the order parameters for $|m| \leq 2$. The dashed red line indicates the time-moment $t_s$ when the final stationary state is selected. After this time moment all order parameters for $m \neq 0$ are decreasing. The data is obtained during the same run as in **Fig. 4** $N = 30$, $K = 0.75$.

Once we have a clear condition for predictability, one can study the average state-selection time $\langle t_s \rangle$, when starting the dynamics from random initial phases $\theta_i$. More precisely, we are interested in how this time depends on the system size $N$ and coupling strength $K$.

The trend as a function of system size for two very different values of $K$ is plotted on Fig. 7. For large enough systems $N \geq 30$ a scaling emerges:

$$\langle t_s \rangle = \alpha(K) \cdot N^{\beta} \tag{33}$$

with $\beta \approx 2.43$.

In the limit of $N = 30$ the trend as a function of the coupling strength, $K$ is plotted on Fig. 8. The results indicate an inverse proportionality between $\langle t_s \rangle$ and $K$:

$$\alpha(K) = \frac{A}{K}, \tag{34}$$

where $A$ is constant. Hence, the selection time $\langle t_s \rangle$ of the final mode $m$ decreases with the coupling strength $K$.

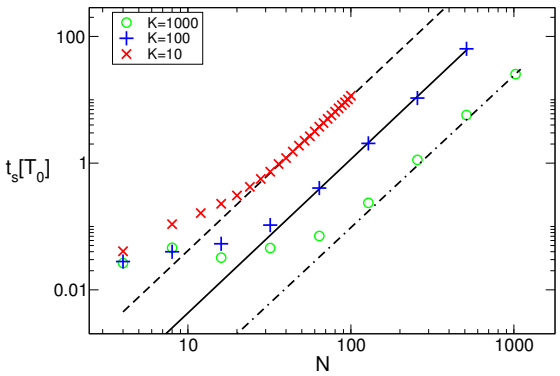


**Figure 7:** (color online) The selection time $\langle t_s \rangle$ as a function of the number of oscillators, $N$. Simulations averaged on several thousands of realizations. Various lines represent power-laws with exponent 2.4.

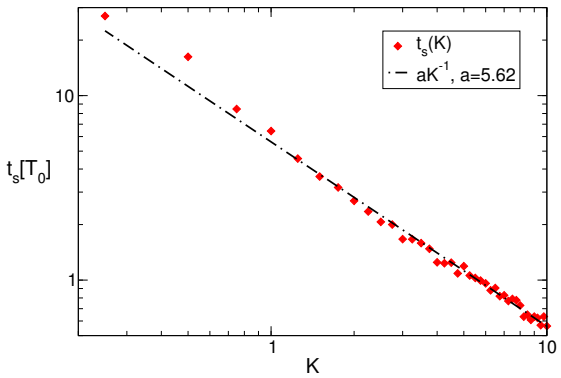


**Figure 8:** (color online) The $\langle t_s \rangle$ selection time as a function of the $K$ coupling intensity between the oscillators. Simulations averaged on several thousands of realizations ($N = 30$).

## Conclusion

Collective oscillation modes were investigated in a ring of identical and locally coupled Kuramoto rotators. Known results were reproduced by using a novel theoretical framework. Our most important result are is that we gave clear conditions for being able to predict the final state of the system. We have shown that the final state of the system is always predictable after a given time-moment, $t_s$.

The final state can be predicted right in the initial state if this is in a compact hypersphere of radius $\epsilon_c(m)$ around the stationary state $m$ with:

$$\epsilon_c(m) \approx 1.7 - \frac{2m\pi}{N}\,. \tag{35}$$

The probability that the initial state is in such domain is very small even for small systems. As the system size increases this probability is exponentially decreasing.

In the most probable case when the system does not start form these compact domains, the dynamics of the generalized Kuramoto order parameters $r_m(t)$ determines the predictability condition. We found that always exists a time moment $t_s$ from where on only one of the order parameters $r_m$ is increasing. At this time moment the final stationary state is predictable. The average value of this time moment, $\langle t_s \rangle$ for random initial phases scales inversely proportional with the coupling strength. For large systems we find that $\langle t_s \rangle$ scales in a nontrivial manner as a function of the system size $N$, with an exponent that is larger than 2.

## Acknowledgement

Work supported from the romanian UEFISCDI grant nr. PN-III-P4-PCE-2016-0363.

# References


[1] Steven H. Strogatz. From Kuramoto to Crawford: exploring the onset of synchronization in populations of coupled oscillators . *Physica D: Nonlinear Phenomena*, 143(1–4):1 – 20, 2000.

[2] A. Pikovsky, M. Rosenblum, and J. Kurths. *Synchronization. A Universal Concept in Nonlinear Sciences*. Cambridge University Press, 2001.

[3] M.J. Panaggio and D.M. Abrams. Chimera states: coexistence of coherence and incoherence in networks of coupled oscillators. *Nonlinearity*, 28(3):R67, 2015.

[4] A. Yeldesbay, A. Pikovsky, and M. Rosenblum. Chimeralike states in an ensemble of globally coupled oscillators. *Phys.Rev. Lett.*, 112:144103, 2014.

[5] J. Wood, T.C. Edwards, and S. Lipa. Rotary traveling-wave oscillator arrays: A new clock technology. *IEEE Journal of Solid-State Circuits*, 36(11):11654–1665, 2001.

[6] Yoshiki Kuramoto. Self-entrainment of a population of coupled non-linear oscillators. In Huzihiro Araki, editor, *International Symposium on Mathematical Problems in Theoretical Physics*, volume 39 of *Lecture Notes in Physics*, pages 420–422. Springer Berlin Heidelberg, 1975.

[7] J.A. Acebrón, L.L. Bonilla, C.J.P. Vicente, F. Ritort, and R. Spigler. The Kuramoto model: A simple paradigm for synchronization phenomena. *Reviews of Modern Physics*, 77(1):137–185, 2005. cited by **739**.

[8] S.H. Strogatz and R.E. Mirollo. Collective synchronisation in lattices of nonlinear oscillators with randomness. *J. Phys. A: Math. Gen.*, 21(1):L699, 1988.

[9] S.H. Strogatz and R.E. Mirollo. Phase locking and critical phenomena in lattices of coupled nonlinear oscillators with random intrinsic frequencies. *Physica D*, 31:143–168, 1988.

[10] B.C. Coutinho, A.V. Goltsev, S.N. Dorogovtsev, and J.F.F. Mendes. Kuramoto model with frequency-degree correlations on complex networks. *Phys. Rev. E.*, 87:031206, 2013.

[11] E.D. Lumer and B.A. Huberman. Hierarchical dynamics in large assemblies of interacting oscillators. *Phys. Lett. A*, 160(1):227–232, 1991.

[12] Daniel A. Wiley, Steven H. Strogatz, and Michelle Girvan. The size of the sync basin. *Chaos: An Interdisciplinary Journal of Nonlinear Science*, 16(1):015103, 2006.

[13] Daido H. Quasientrainment and slow relaxation in a population of oscillators with random and frustrated interactions. *Phys. Rev. Lett.*, 68:1073, 1992.

[14] M. K. Stephen Yeung and Steven H. Strogatz. Time delay in the Kuramoto model of coupled oscillators. *Phys. Rev. Lett.*, 82:648–651, Jan 1999.

[15] M.G. Earl and S.H. Strogatz. Synchronization in oscillator networks with delayed coupling: A stability criterion. *Phys. Rev. E*, 67:036204, 2003.

[16] Sethia. G.C., A. Sen, and F.M. Atay. Clustered chimera states in delay-coupled oscillator systems. *Phys. Rev. Lett.*, 100:144102, 2008.

[17] A. Lahiri T. K. Roy. Synchronized oscillations on a Kuramoto ring and their entrainment under periodic driving . *Chaos, Solitons & Fractals*, 45(6):888 – 898, 2012.

[18] Ramana Dodla, Abhijit Sen, and George L. Johnston. Phase-locked patterns and amplitude death in a ring of delay-coupled limit cycle oscillators. *Phys. Rev. E*, 69:056217, May 2004.

[19] Robert M. Gray. Toeplitz and Circulant Matrices: A Review. *Foundations and Trends® in Communications and Information Theory*, 2(3):155–239, 2005.